Research Square

Preprints are preliminary reports that have not undergone peer review.
They should not be considered conclusive, used to inform clinical practice,
or referenced by the media as validated information.

Extension of In-Gap Electronic-State Spectrum Extraction Technique Based on Transient Photo-Voltage Measurement

Zedong Lin (zedonglin@ruc.edu.cn)
Renmin University of China

Research Article

Keywords: photo-voltage, experimental, TPV

Posted Date: March 3rd, 2021

DOI: https://doi.org/10.21203/rs.3.rs-258102/v1

License: This work is licensed under a Creative Commons Attribution 4.0 International License.
Read Full License

Extension of in-gap electronic-state spectrum extraction technique based on transient photo-voltage measurement

Zedong Lin*

E-mail: zedonglin@ruc.edu.cn

Department of Chemistry, Renmin University of China, Beijing 100872, China.

ABSTRACT

This article puts forward a novel insight for extraction of trap state density (DOS_T) based on the transient photo-voltage (TPV) experimental data. Inspired by the method based on the Gauss distribution model, we introduce a universal general distribution model and present a general technique of DOS_T distribution from the experimental data of TPV measurement. The method based on the exponential (Gauss) distribution model is the one (two) order special case of our method. Compared to the method based on the exponential model (applicable only when the TPV result satisfies linear relation) and Gauss model (applicable only when the TPV result satisfies quadratic function relation), our work is effective for arbitrary TPV result.

Introduction

The density of trap states (DOS_T) distribution is one of the most important factors determining the power conversion efficiency (PCE) of perovskite solar cells (PSCs)[1-6]. It affects the carrier recombination and transport to hinder the enhancement of PCE[7-

[10]. Recent years, people focus on the study of trap passivation[1-5]. Trap passivation reduces the amount of trap states to improve the PCE. To evaluate the passivation efficiency, we need to calculate the DOS_T distributions of devices with and without passivation for compare[1,2,4,6]. There are few breakthroughs made in the DOS_T extraction. The method based on the temperature-dependent space-charge limited current (SCLC) theory extracts the DOS_T distribution from the experimental data of SCLC measurement[11-17]. Using the equivalent chemical capacitance model, Walter et al. put forward the DOS_T extraction technique based on the impedance spectroscopy data (IS)[18-22]. Lin put forward the time-resolved charge extraction (TRCE) method[23]. Wang et al. presented the transient photo-voltage (TPV) method for DOS_T extraction[24-28]. They consider the DOS_T distribution of PSCs satisfies the exponential type. Based on the exponential distribution model[24-27], multiple-trapping model[29,30] and zero-temperature approximation[28], they predicted that the TPV result is linear. However, their prediction is not consistent with the result of TPV measurement. The TPV experimental measurement shows the non-linear result[24-27]. To solve this difficulty, Lin gave up the exponential distribution model and introduced the Gauss distribution model to replace it[31]. The prediction made by his

theory shows that the TPV result satisfies quadratic function relation, which is in line with the TPV measurement[31]. Inspired by the theory given by Lin, in this paper, we introduce a general distribution function to extend his method. We successfully put forward a general extraction method of DOS_T distribution. The method based on the exponential distribution model is the one order special case of our method. In the two order special case, our method come back to the theory given by Lin.

Results

Exponential type distribution theory. The method given by Wang et al. shows that the DOS_T distribution satisfies $\rho_{\mathrm{trap}}(E) = \frac{N_T}{E_B} exp\left(\frac{E-E_c}{E_B}\right)$. Here, N_T denotes the density of trap states. E_B denotes the characteristic energy. E_c denotes the conduction band minimum[24-28]. They predicted that TPV result is linear, which satisfies

$$\ln \tau_n = AV_{ph} + B \qquad (1)$$

Here,

$$A = e/E_B - e/k_B T, \qquad (2)$$

$$B = (E_{Fp}-E_c)/E_B - (E_{Fp}-E_c)/k_B T + \ln(N_T k_B T \tau_f / N_c E_B). \qquad (3)$$

e denotes the elementary charge. k_B is the Boltzmann constant. T is the ambient temperature. E_{Fp} is the hole quasi Fermi energy level. N_c is the conduction band DOS. τ_f is the free carrier

lifetime[24-28].

Taking the TPV data in refs 25 as an example, as shown in Figure 1 (a), we made a linear fitting for the TPV result. According to the fitting coefficients A and B of fitting function $f(V_{ph})=AV_{ph}+B$ and formula (2), (3), we calculate the parameters of E_B and N_T to determine the DOS_T distribution (Figure 1 (b)).

However, Figure 1(a) shows that the TPV result is consistent badly with the linear fitting, indicating that the DOS_T distribution extracted by their method is not accurate.

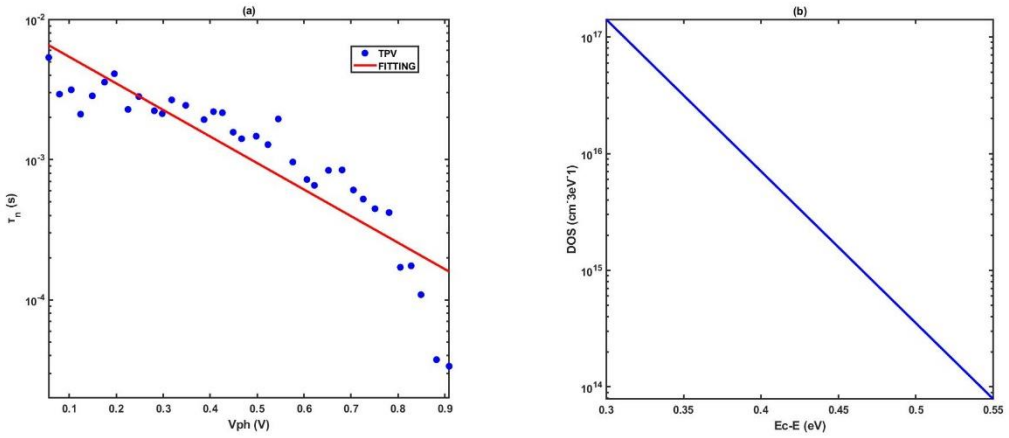

Figure 1. (a) Linear fitting of the TPV experimental result. (b) DOS_T distribution extracted by the method given by Wang et al.

Gauss type distribution theory. Lin consider the DOS_T distribution satisfies the Gauss type distribution ($\rho_{trap}(E) = \frac{N_T}{\sigma\sqrt{2\pi}} exp\left(-\frac{(E-E_c)^2}{2\sigma^2}\right)$). Here, σ is the distribution parameter. He predicted that the logarithm of carrier lifetime is a quadratic

function of the photo-voltage, which satisfies Lin's equation[31]

$$ln\tau_{\mathrm{n}} = AV_{\mathrm{ph}}^2 + BV_{\mathrm{ph}} + C, \qquad (4)$$

Here,

$$A = -\frac{e^2}{2\sigma^2}, \qquad (5)$$

$$B = \frac{E_{\mathrm{c}}e}{\sigma^2} - \frac{e}{k_{\mathrm{B}}T} - \frac{E_{\mathrm{Fp}}e}{\sigma^2}, \qquad (6)$$

$$C = -\frac{E_{\mathrm{Fp}}^2}{2\sigma^2} + \left(\frac{E_{\mathrm{c}}}{\sigma^2} - \frac{1}{k_{\mathrm{B}}T}\right)E_{\mathrm{Fp}} + \frac{2\sigma^2E_{\mathrm{c}} - k_{\mathrm{B}}TE_{\mathrm{c}}^2}{2\sigma^2k_{\mathrm{B}}T} + ln\left(\frac{N_{\mathrm{T}}k_{\mathrm{B}}T\tau_{\mathrm{f}}}{\sigma\sqrt{2\pi}N_{\mathrm{c}}}\right). \qquad (7)$$

Making a quadratic function fitting for the TPV result (Figure 2(a)), we obtain the fitting coefficients *A*, *B*, *C* of fitting function $\mathrm{f}(V_{\mathrm{ph}}) = AV_{\mathrm{ph}}^2 + BV_{\mathrm{ph}} + C$. It shows that the TPV result is consistent with the quadratic function fitting. According to the formula (3) and (5), we calculate the parameters of Gauss distribution (σ, N_{T}) to determine the $\mathrm{DOS_T}$ distribution (Figure 2 (b)). [31]

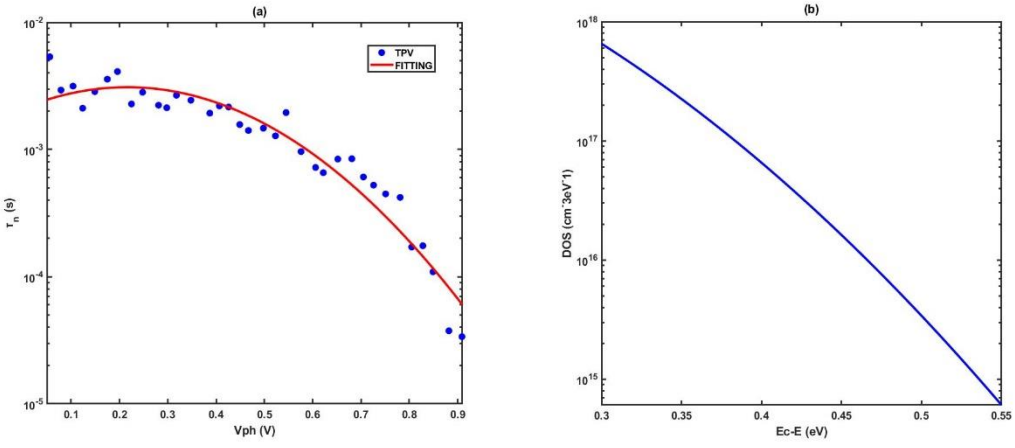

Figure 2. (a) Quadratic function fitting of the TPV result. (b) $\mathrm{DOS_T}$ distribution extracted by the method given by Lin. Panels

are reproduced from refs 31.

Extension of Lin's method. Inspired by Lin's method, we try to extend his method. We suppose the DOS_T distribution satisfies the distribution form

$$\rho_{\mathrm{trap}}(E) = (N_{\mathrm{T}}/\varepsilon) exp\left((-1)^{n+1}\frac{(E-E_{\mathrm{c}})^n}{\varepsilon}\right), \quad (8)$$

Here, $n \in N^*$. N^* denotes the set of positive integers. N_T and ε are the distribution parameters. Because the parameter ε has the property of energy, we define $\varepsilon > 0$. Based on this distribution function, we make prediction for TPV result. The density of electron in traps satisfies the formula[31,32]

$$n_{\mathrm{t}} = \int_{E_{\mathrm{v}}}^{E_{\mathrm{c}}} \rho_{\mathrm{trap}}(E) f(E)\, dE \quad (9)$$

Here, $f(E)$ is the Fermi-Dirac distribution[31,32].

Making the zero-temperature approximation[28], we have

$$n_{\mathrm{t}} = \int_{E_{\mathrm{v}}}^{E_{\mathrm{Fn}}} (N_{\mathrm{T}}/\varepsilon) exp\left((-1)^{n+1}\frac{(E-E_{\mathrm{c}})^n}{\varepsilon}\right) dE. \quad (10)$$

Therefore, we have

$$\frac{\partial n_{\mathrm{t}}}{\partial E_{\mathrm{Fn}}} = (N_{\mathrm{T}}/\varepsilon) exp\left((-1)^{n+1}\frac{(E_{\mathrm{Fn}}-E_{\mathrm{c}})^n}{\varepsilon}\right). \quad (11)$$

The electron density in conductor band satisfies[32]

$$n_{\mathrm{c}} = N_{\mathrm{c}} exp\left(\frac{E_{\mathrm{Fn}}-E_{\mathrm{c}}}{k_{\mathrm{B}}T}\right), \quad (12)$$

Therefore, we have

$$\frac{\partial n_{\mathrm{c}}}{\partial E_{\mathrm{Fn}}} = \frac{N_{\mathrm{c}}}{k_{\mathrm{B}}T} exp\left(\frac{E_{\mathrm{Fn}}-E_{\mathrm{c}}}{k_{\mathrm{B}}T}\right). \quad (13)$$

Adopting the approximation of $n \approx n_t$[29], we write the multiple-trapping model $\tau_n = (\partial n/\partial n_c)\,\tau_f$ [29,30]as $\tau_n = (\partial n_t/\partial n_c)\,\tau_f$.

Therefore, we have

$$\tau_{\mathrm{n}} = \frac{\partial n_{\mathrm{t}}/\partial E_{\mathrm{Fn}}}{\partial n_{\mathrm{c}}/\partial E_{\mathrm{Fn}}}\tau_{\mathrm{f}} \qquad (14)$$

According to the formula (11), (13), (14) and the relation of $E_{\mathrm{Fn}}=E_{\mathrm{Fp}}+V_{\mathrm{ph}}e$[32], we have

$$ln\tau_{\mathrm{n}} = \sum_{l=0}^{n} A_l V_{\mathrm{ph}}^{l}, \qquad (15)$$

Here,

$$A_l = (-1)^{n+1}\frac{C_n^l e^l (E_{\mathrm{Fp}}-E_{\mathrm{c}})^{n-l}}{\varepsilon}, \qquad l=2,\ldots\ldots,n. \qquad (16)$$

$$A_1 = \frac{ne(E_{\mathrm{Fp}}-E_{\mathrm{c}})^{n-1}}{\varepsilon} - \frac{e}{k_{\mathrm{B}}T}, \qquad (17)$$

$$A_0 = -\frac{(E_{\mathrm{Fp}}-E_{\mathrm{c}})^{n}}{\varepsilon} - \frac{E_{\mathrm{Fp}}-E_{\mathrm{c}}}{k_{\mathrm{B}}T} + ln\left(\frac{N_{\mathrm{T}}k_{\mathrm{B}}T\tau_{\mathrm{f}}}{\varepsilon N_{\mathrm{c}}}\right). \qquad (18)$$

For intrinsic perovskite, the quasi Fermi energy level satisfies $E_{\mathrm{Fn}}=E_{\mathrm{F0}}+V_{\mathrm{ph}}e/2$[32]. We have

$$A_l = (-1)^{n+1}\frac{C_n^l e^l (E_{\mathrm{F0}}-E_{\mathrm{c}})^{n-l}}{2^l\varepsilon}, \qquad l=2,\ldots\ldots,n. \qquad (19)$$

$$A_1 = \frac{ne(E_{\mathrm{F0}}-E_{\mathrm{c}})^{n-1}}{2\varepsilon} - \frac{e}{2k_{\mathrm{B}}T}, \qquad (20)$$

$$A_0 = -\frac{(E_{\mathrm{F0}}-E_{\mathrm{c}})^{n}}{\varepsilon} - \frac{E_{\mathrm{F0}}-E_{\mathrm{c}}}{k_{\mathrm{B}}T} + ln\left(\frac{N_{\mathrm{T}}k_{\mathrm{B}}T\tau_{\mathrm{f}}}{\varepsilon N_{\mathrm{c}}}\right). \qquad (21)$$

Equation (15) is the fundamental equation of our extension method. It shows that the logarithm of carrier lifetime is a polynomial function of the photo-voltage. This prediction is consistent with TPV measurement, indicating that the introduced distribution function (equation (8)) is reliable. Obviously, the method given by Wang et al. is the special case of our extension method (n=1). Lin's method is the special case of our extension method (n=2).

Making a polynomial function fitting for the TPV result, we get values of parameters A_l (l=0,……,n). According to the formula (29-31), we calculate the distribution parameters (N_T and ε) to obtain DOS_T distribution. The parameters used for calculation are cited from refs 7.

Taking the TPV data in refs 25 as an example, we make polynomial fittings for the TPV result (Figure 3(a-e)). The blue dots represent the TPV data. The red solid lines represent the polynomial fittings for the TPV data. It shows that the R-square (coefficient of determination) increases with increasing n (Figure 3(f)), indicating that the fitting coincidence degree improves with increasing n.

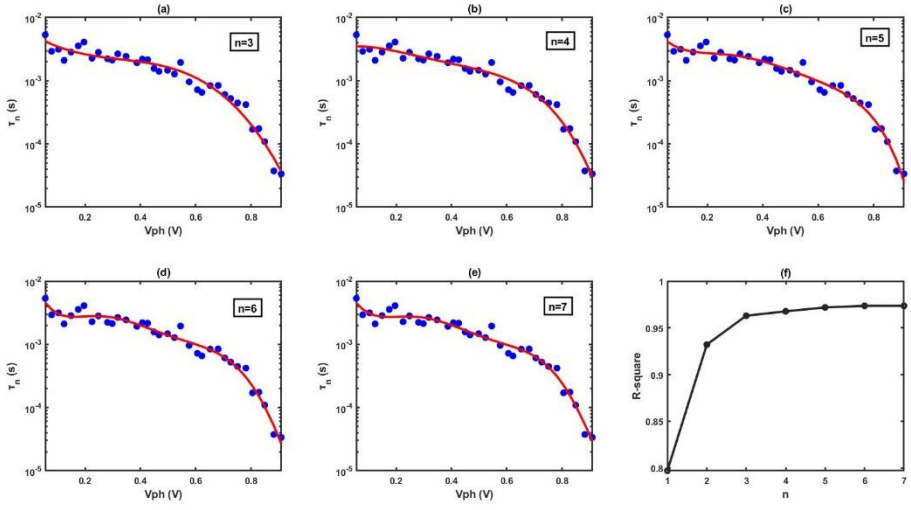

Figure 3. (a-e) Polynomial fittings for TPV experimental result. (f) Plot of n versus R-square.

By using our method, we calculate the distribution

parameters (ε and N_T) for the cases of n=1~7. The coefficients of polynomial fitting and distribution parameters are listed in Table 1. The cases of n=1, 2, 4, 7 satisfies the definition of ε>0, so the DOS_T distribution extracted at these cases are reliable. The extracted DOS_T distribution at these cases are shown in Figure 1(b) (exponential type distribution n=1), Figure 2(b) (Gauss type distribution n=2), Figure 4 (a) (n=4), Figure 4 (b) (n=7), respectively.

Table 1. Fitting coefficients, fitting errors and distribution parameters

Coefficients	exp	Gauss	n=3	n=4	n=5	n=6	n=7
A_1	-4.36	-7.93	-17.24	-29.98	-131.9	374	400.7
A_2	-4.79	3.23	16.9	40.56	287.9	-1215	-976.6
A_3		-6.09	-6.69	-19.97	-237.7	1497	612.5
A_4			-5.14	1.99	87.04	-890.2	228.9
A_5				-5.71	-15.17	261.3	-412
A_6					-4.86	-36.06	165.8
A_7						-4.04	-27.05
A_8							-4.34
R-square	0.7971	0.9321	0.963	0.9677	0.9719	0.9736	0.9736
ε (eV)	E_B=0.03	σ=0.12	-1.9×10^{-40}	8.5×10^{-60}	-1.6×10^{-79}	-4.4×10^{-99}	3.3×10^{-118}
N_T (cm^{-3})	3.8×10^{19}	3.9×10^{18}	-4.2×10^{-19}	1.1×10^{-38}	-4.6×10^{-58}	-3.0×10^{-77}	1.7×10^{-96}

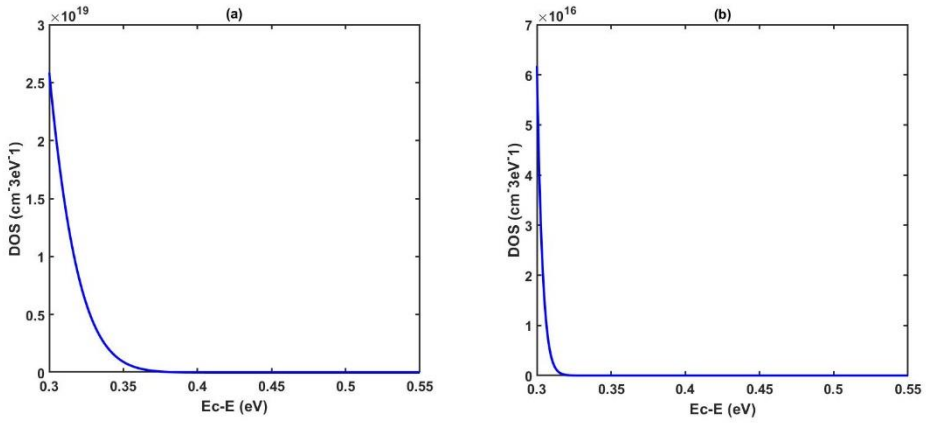

Figure 4. DOS_T distributions extracted by our method at different polynomial fitting degrees. (a) n=4. (b) n=7.

According to the R-square of polynomial fittings, the coincidence degree of fitting increases with increasing n. However, when the value of n is too large, the fitting result carries some noises. Therefore, it does not mean that the accurate of extracted DOS_T distribution with increasing value of n. To extract the reliable DOS_T distribution, we need to choose suitable polynomial fitting degree to ensure the coincidence degree of fitting is high enough and carries little noises.

Calculation Example. For further investigation, we take the TPV date in refs 26 as example. Figure 5 shows the TPV data for a photovoltaic device with perovskite active layer of $MA_{0.4}FA_{0.6}PbI_3$. The blue dots represent the TPV data. The red lines represent the polynomial fittings for the TPV data. We make

Polynomial fitting for the TPV data at different polynomial fitting degrees (n=1~6). The corresponding coefficients are listed in Table 2.

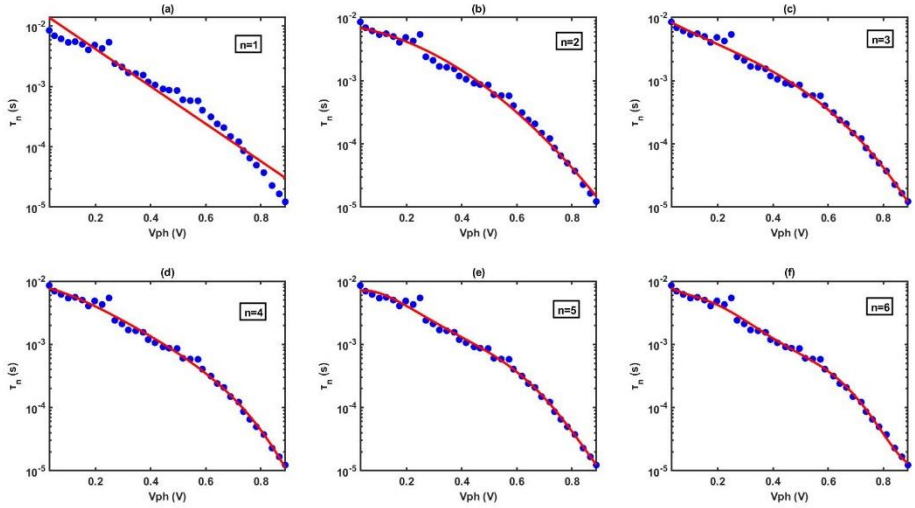

Figure 5. Polynomial fitting of TPV result at different polynomial fitting degrees (n=1~6).

Table 2. Fitting coefficients, fitting errors and distribution parameters

Coefficients	exp	Gauss	n=3	n=4	n=5	n=6
A_1	-7.14	-6.03	-7.12	-13.65	67.57	379.5
A_2	-4.05	-1.61	3.78	18	-169.1	-979.7
A_3		-4.92	-5.28	-11.27	146.5	935.2
A_4			-4.61	-2.07	-56.96	-408.4
A_5				-4.79	4.41	77.57
A_6					-5.04	-9.52
A_7						-4.61
R-square	0.9554	0.9907	0.9932	0.9937	0.9942	0.9949
ε (eV)	E_B=0.041	0.14	-4.49×10^{-40}	1.87×10^{-59}	3.3×10^{-79}	-4.31×10^{-99}
N_T (cm^{-3})	2.27×10^{18}	1.39×10^{19}	-1.72×10^{-18}	6.05×10^{-38}	7.61×10^{-58}	-1.65×10^{-77}

We choose the polynomial fitting which satisfies the definition of ε>0 to extract the DOS_T distribution. Because the

TPV result obviously deviates the linear relation (Figure 5(a)), the DOS_T distribution extracted by Wang et al is not reliable (Figure 6(a)). The fitting effect by Lin's method is better than the method given by Wang et al, the DOS_T distribution extracted by Lin' method is more reliable (Figure 6(b)). Because the fitting coincidence degree at the polynomial fitting degree of 4 and 5 is much higher, the extracted DOS_T distributions shown in Figure 6(c) and (d) are more accurate.

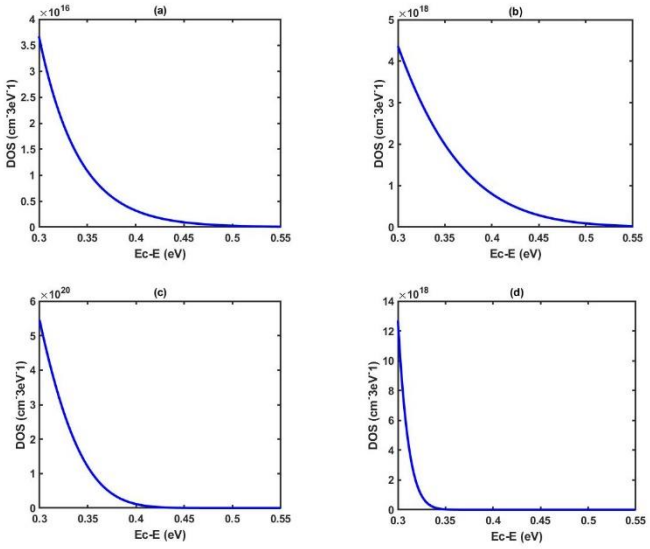

Figure 6. (a) DOS_T distributions extracted by the method given by Wang et al. (b) DOS_T distribution extracted by Lin's method. (c) (d) DOS_T distribution extracted by our method at the polynomial fitting degree of 4 and 5, respectively.

Conclusion

In summary, inspired by the Lin's method, we introduce a general DOS_T distribution function. By Strict mathematical derivation,

we proof that the logarithm of carrier lifetime is a polynomial function of the photo-voltage. Our method successfully extend Lin's method. The method presented in this paper is effective for arbitrary TPV result (not only effective for the case of linear or quadratic function relation TPV result). Our work gives a complete set of DOS_T distribution extraction method.

Acknowledgements

I am grateful to Ning-Hua Tong and Xin-Gui Tang for their helpful comments. In addition, I especially wishes to thank my girlfriend Luren Zhang, who give me powerful spiritual support.

Author contributions

Zedong Lin finishes the whole work of this paper.

Competing interests

The author declares no competing interests.

References

1. Zhao, Y. *et al*. Molecular interaction regulates the performance and longevity of defect passivation for metal halide perovskite solar cells. *J. Am. Chem. Soc.* **142**, 20071-20079 (2020).
2. Azmi, R. *et al*. Shallow and deep trap state passivation for low-temperature processed perovskite solar cells. *ACS Energy Lett.* **5**, 1396-1403 (2020).
3. Yang, B. *et al*. Outstanding passivation effect by a mixedsalt interlayer with internal interactions in perovskite solar cells. *ACS Energy Lett.* **5**, 3159-3167 (2020).
4. Wang, G. *et al*. In situ passivation on rear perovskite interface for efficient and stable perovskite solar cells. *ACS Appl. Mater. Interfaces* **12**, 7690-7700 (2020).
5. Long, J. *et al*. Understanding the mechanism between antisolvent dripping and additive doping strategies on the passivation effects in perovskite solar cells. *ACS Appl. Mater. Interfaces* **12**, 56151-56160 (2020).
6. Xue, J., Wang, R. & Yang, Y. The surface of halide perovskites from nano to bulk. *Nat. Rev. Mater.* **5**, 809-827 (2020).

7. Lin, Z. Extraction technique of trap states based on transient photo-voltage measurement. *Sci. Rep.* **10**, 12888 (2020).
8. Calado, P. *et al*. Identifying dominant recombination mechanisms in perovskite solar cells by measuring the transient ideality factor. *Phys. Rev. Appl*. **11**, 044005 (2019).
9. Ran, C., Xu, J., Gao, W., Huang, C. & Dou, S. Defects in metal triiodide perovskite materials towards high-performance solar cells: origin, inpact, characterization, and engineering. *Chem. Soc. Rev*. **47**, 4581 (2018).
10. Lakhwani, G., Rao, A. & Friend, R. H. Bimolecular recombination in organic photovoltaics. *Annu. Rev. Phys. Chem*. **65**, 557-581 (2014).
11. Ball, J. M. & Petrozza, A. Defects in perovskite-halides and their effects in solar cells. *Nat. Energy* **1**, 16149 (2016).
12. Adinolfi, V. *et al*. The in-gap electronic state spectrum of methylammonium lead iodide single-crystal perovskites. *Adv. Mater.* **28**, 3406-3410 (2016).
13. Schauer, F., Novotny, R. & Nešpůrek, S. Space-charge-limited-current spectroscopy: possibilities and limitations. *J. Appl. Phys*. **81**, 1244-1249 (1997).
14. Dacuña, J. & Salleo, A. Modeling space-charge-limited currents in organic semiconductors: extracting trap density and mobility. *Phys. Rev. B* **84**, 195209 (2011).
15. Schauer, F., Nešpůrek, S. & Valerian, H. Temperature dependent space-charge-limited currents in amorphous and disordered semiconductors. *J. Appl. Phys*. **80**, 880-888 (1996).
16. Pospisil, J. *et al*. Density of bulk trap states of hybrid lead halide perovskite single crystals: temperature modulated space-charge-limited-current. *Sci. Rep*. **9**, 3332 (2019).
17. Krellner, C. *et al*. Density of bulk trap states in organic semiconductor crystals: discrete levels induced by oxygen in rubrene. *Phys. Rev. B* **75**, 245115 (2007).
18. Walter, T., Herberholz, R., Müller, C. & Schock, H. W. Determination of defect distributions from admittance measurements and application to Cu(In, Ga)Se_2 based heterojunctions. *J. Appl. Phys*. **80**, 4411-4420 (1996).
19. Duan, H. *et al*. The identification and characterization of defect states in hybrid organic-inorganic perovskite photovoltaics. *Phys. Chem. Chem. Phys*. **17**, 112-116 (2015).
20. von Hauff, E. Impedance spectroscopy for emerging photovoltaics. *J. Phys. Chem.*

C **123**, 11329-11346 (2019).

21. Lee, B. *et al*. Aminosilane-modified CuGaO2 nanoparticles incorporated with CuSCN as a hole-transport layer for efficient and stable perovskite solar cells. *Adv. Mater. Interfaces* **6**, 1901372 (2019).
22. Hwang, T. *et al*. Electronic traps and their correlations to perovskite solar cell performance via compositional and thermal annealing controls. *ACS Appl. Mater. Interfaces* **11**, 6907-6917 (2019).
23. Lin, Z. New extraction technique of in-gap electronic-state spectrum based on time-resolved charge extraction. *ACS Omega* **5**, 21762-21767 (2020).
24. Wang, Y. *et al*. Correlation between energy and spatial distribution of intragap trap states in the TiO_2 photoanode of dye-sensitized solar cells, *ChemPhysChem.* **16**, 2253-2259 (2015).
25. Wang, H. *et al*. Mechanism of biphasic charge recombination and accumulation in TiO_2 mesoporous structured perovskite solar cells, *Phys. Chem. Chem. Phys.* **18**, 12128 (2016).
26. Zhao, J. *et al*. Charge carrier recombination dynamics in a bi-cationic perovskite solar cell. *Phys. Chem. Chem. Phys.* **21**, 5409 (2019).
27. Wang, H. *et al*. Adverse effects of excess residual PbI2 on photovoltaic performance charge separation and trap-state properties in mesoporous structured perovskite solar cells, *Chem. Eur. J.* **23**, 3986-3992 (2017).
28. Wang, H. *et al*. Multiple-trapping model for the charge recombination dynamics in mesoporous-structured perovskite solar cells, *ChemSusChem.* **10**, 4872-4878 (2017).
29. Bisquert, J. & Vikhrenko, V. S. Interpretation of the time constants measured by kinetic techniques in nanostructured semiconductor electrodes and dye-sensitized solar cells, *J. Phys. Chem. B* **108**, 2313 (2004).
30. Bisquert, J., Fabregat-Santiago, F., Mora-Seró, I., Belmonte, G. G. & Giménez, S. Electron lifetime in dye-sensitized solar cells: theory and interpretation of measurements, *J. Phys. Chem. C* **113**, 17278-17290 (2009).
31. Lin, Z. A more accurate calculation method of trap state distribution based on transient photo-voltage measurement. *Chemical Physics* **542**, 111070 (2021).
32. Nelson, J. The physics of solar cells (Imperial College Press, London, 2003).

Figures

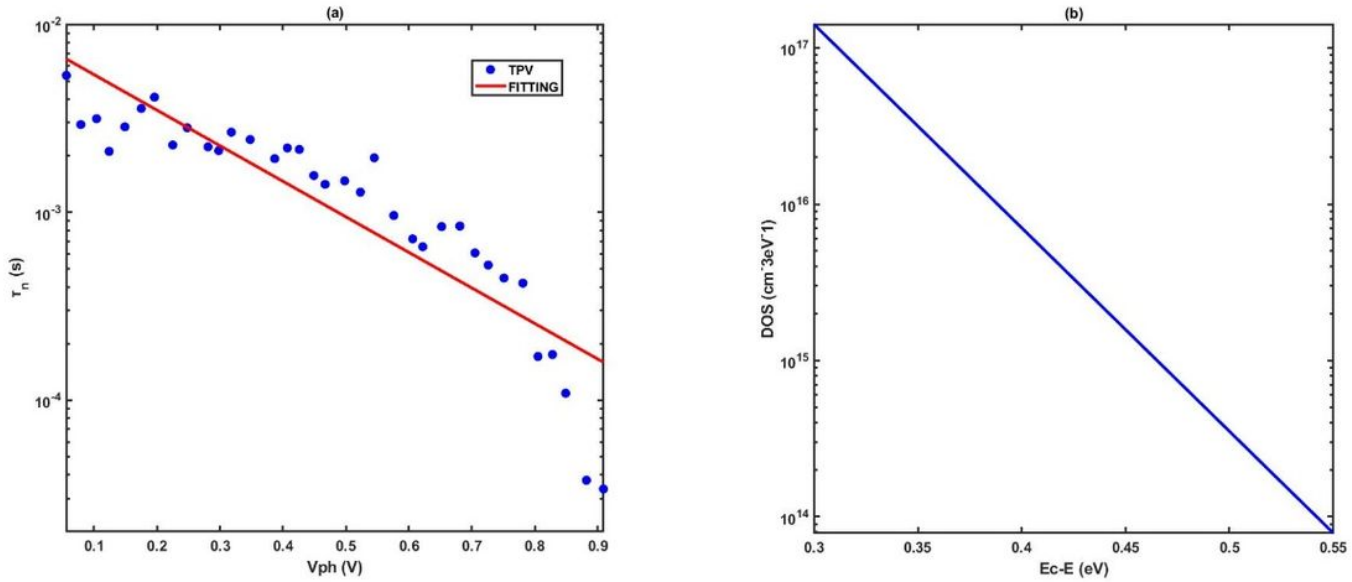

Figure 1

(a) Linear fitting of the TPV experimental result. (b) DOST distribution extracted by the method given by Wang et al.

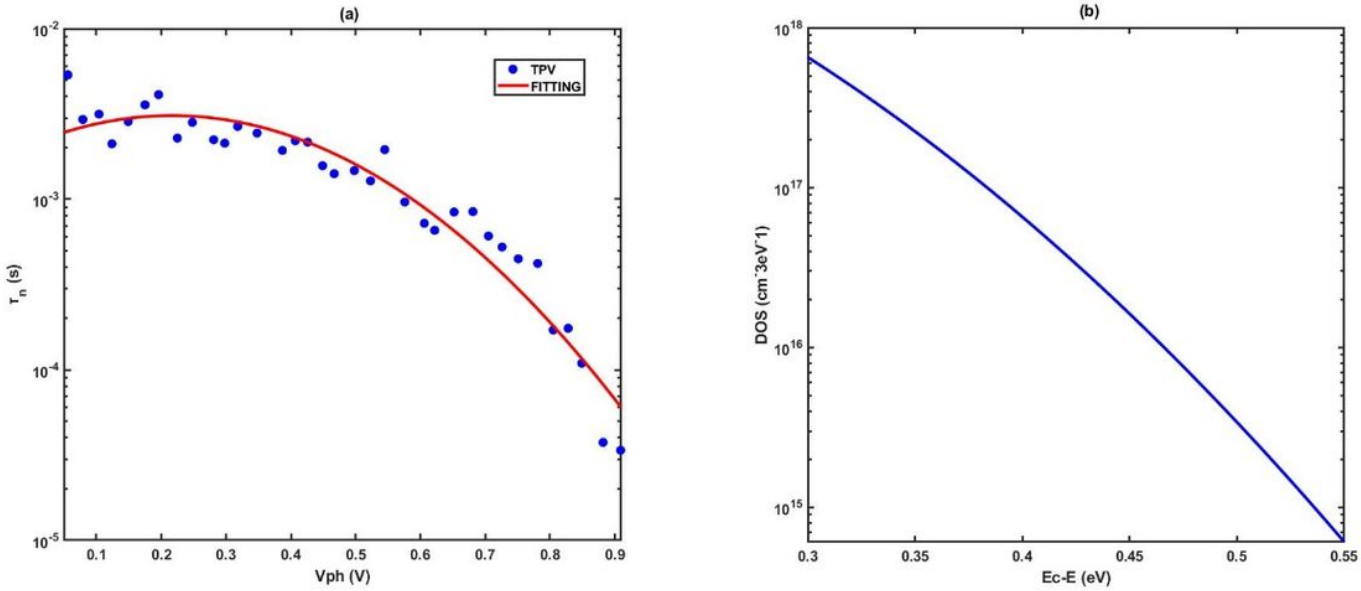

Figure 2

(a) Quadratic function fitting of the TPV result. (b) DOST distribution extracted by the method given by Lin. Panels are reproduced from refs 31.

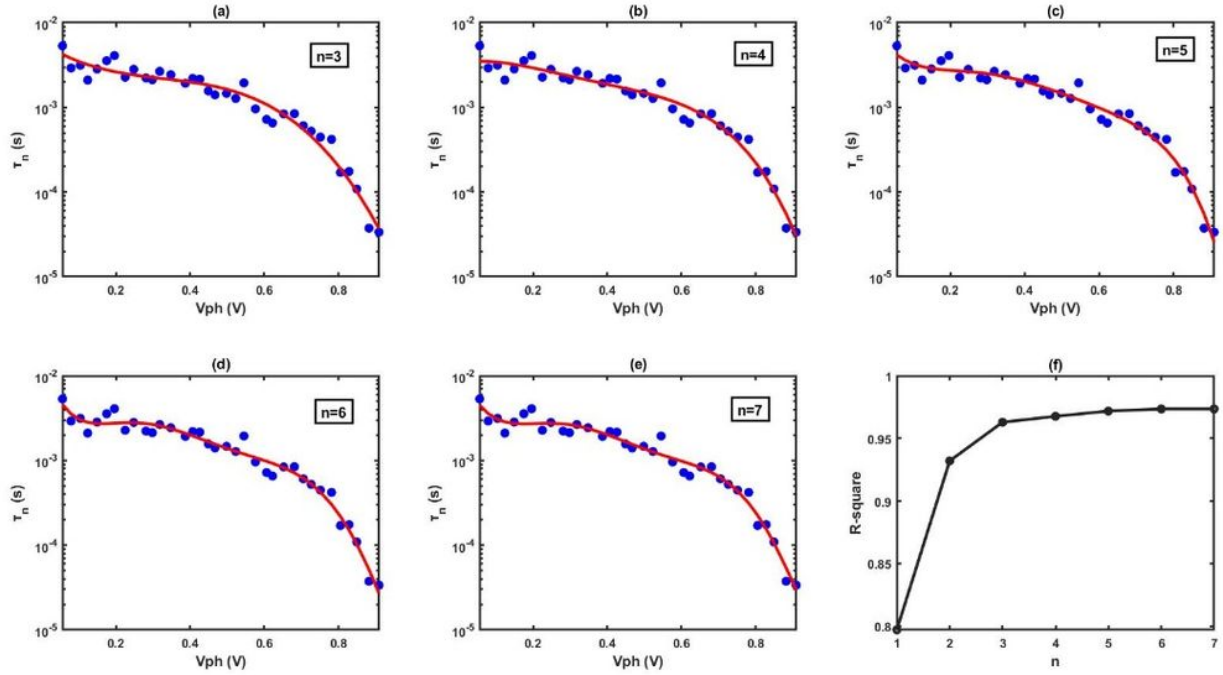

Figure 3

(a-e) Polynomial fittings for TPV experimental result. (f) Plot of n versus R-square.

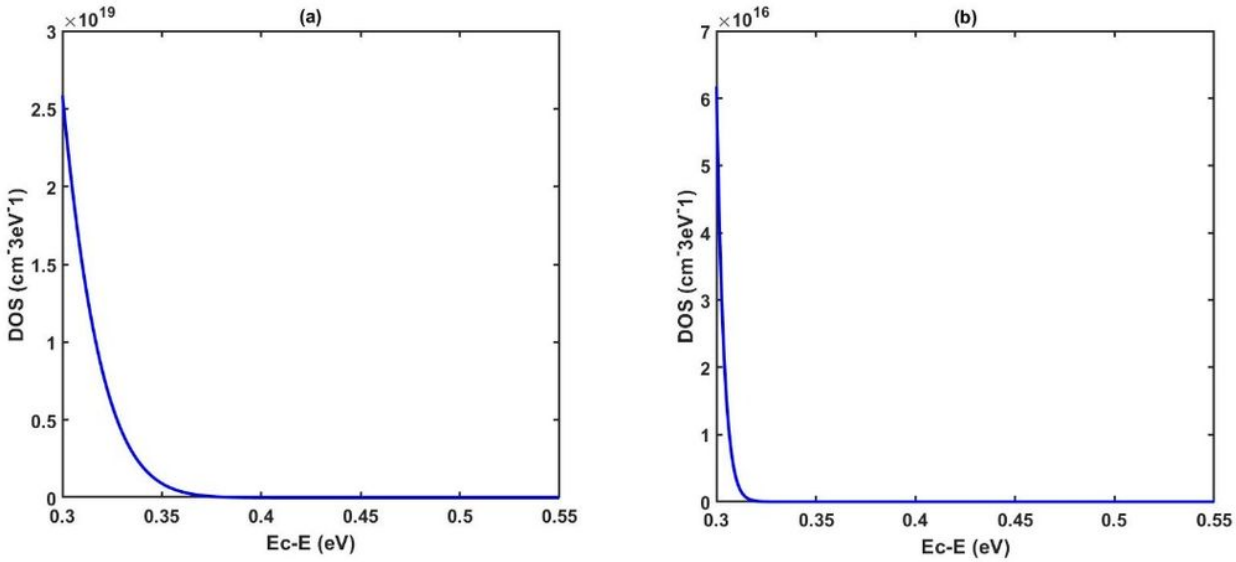

Figure 4

DOST distributions extracted by our method at different polynomial fitting degrees. (a) n=4. (b) n=7.

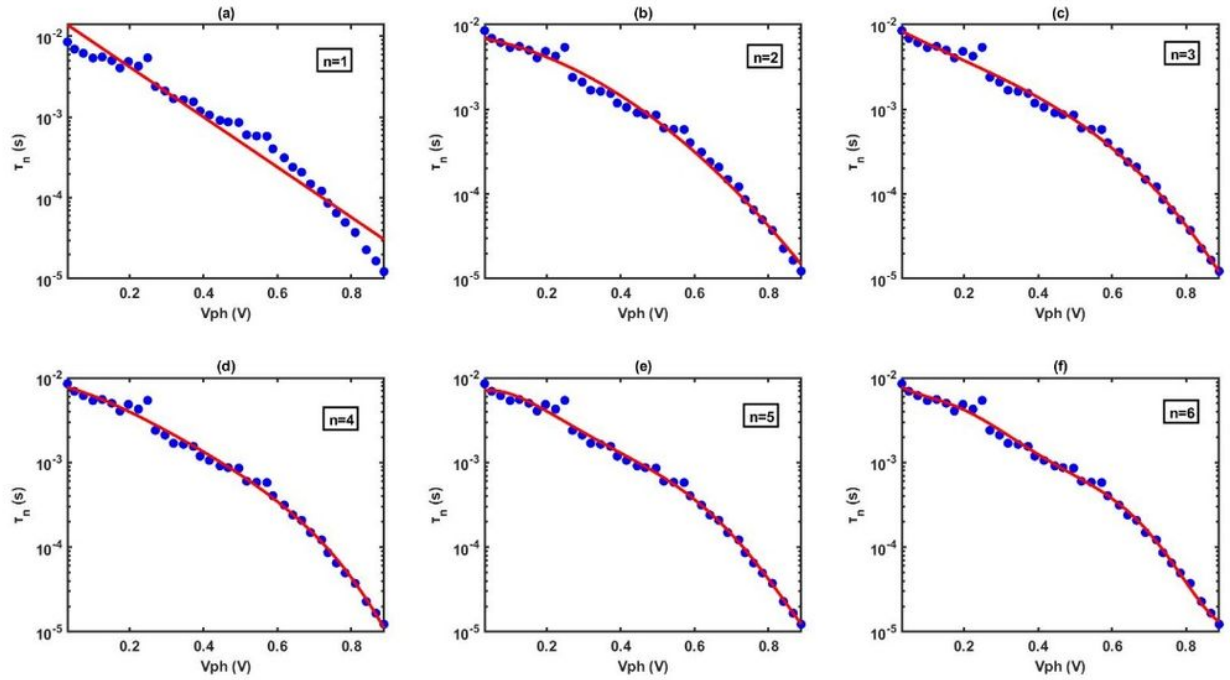

Figure 5

Polynomial fitting of TPV result at different polynomial fitting degrees (n=1~6).

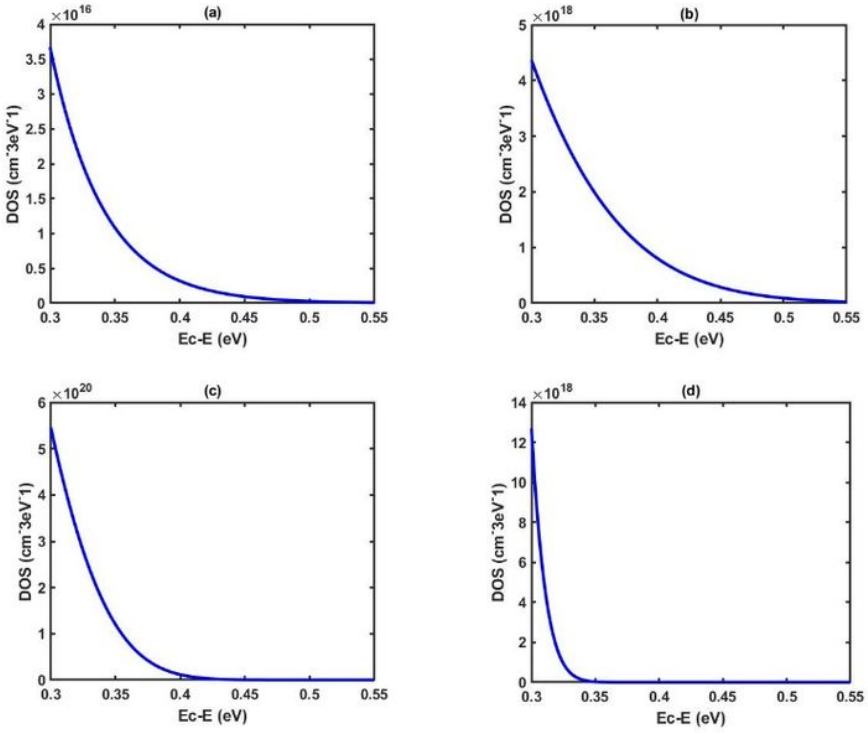

Figure 6

(a) DOST distributions extracted by the method given by Wang et al. (b) DOST distribution extracted by Lin's method. (c) (d) DOST distribution extracted by our method at the polynomial fitting degree of 4 and 5, respectively.